Strål säkerhets myndigheten
Swedish Radiation Safety Authority

Author: Magnus Dahlberg
Dave Hannes

Research

2016:27

Validation of fatigue fracture mechanics approaches

Report number: 2016:27 **ISSN:** 2000-0456
Available at www.stralsakerhetsmyndigheten.se

SSM perspective

Background

In a previous study (SSM research report 2015:38) fatigue experiments were performed on welded austenitic stainless steel piping components. The fatigue experiments offer an opportunity to evaluate fatigue flaw tolerance assessments used in industry, which are based on the fracture mechanical approach implemented in ProSACC.

Objective

The present study aims to validate the used fatigue flaw tolerance approaches by comparing experimental results obtained for the total fatigue life of the considered piping component and the computed fatigue life estimate. Safe and reliable long term operation (LTO) of the plant has to be demonstrated when NPPs approach the end of their design service life time, and this process includes amongst others the evaluation of fatigue resistance of components.

Results

The study indicates that an ASME inspired flaw tolerance approach causes extensive conservatism, implying that the propagation fatigue life at most represents 10% of the total fatigue life. A best-estimate flaw tolerance approach on the other hand presents a significant reduction of conservatism, which indicates that fatigue initiation represents a negligible contribution to the total fatigue life. The estimated 90% prediction limits of the best-estimate approach show good agreement with the experimental results. Overall conservatism of the fatigue flaw tolerance approach is preserved by assuming a relatively large initial flaw size and neglecting effects from inelastic material behaviour, sequence effects for variable amplitude loads and crack closure effects.

The results support the use of flaw tolerance approaches for demonstrating reliability of a component.

Project information

Contact person SSM: Fredrik Forsberg
Reference: SSM2015-3855

Strål
säkerhets
myndigheten
Swedish Radiation Safety Authority

Author: Magnus Dahlberg, Dave Hannes
Inspecta Technology AB, Stockholm, Sweden

2016:27

Validation of fatigue fracture mechanics approaches

Date: September 2016
Report number: 2016:27 **ISSN:** 2000-0456
Available at www.stralsakerhetsmyndigheten.se

This report concerns a study which has been conducted for the Swedish Radiation Safety Authority, SSM. The conclusions and viewpoints presented in the report are those of the author/authors and do not necessarily coincide with those of the SSM.

Title: Validation of fatigue fracture mechanics approaches
Author: Dave Hannes, Magnus Dahlberg
Inspecta Technology AB,
Stockholm Sweden
Date: 2016-08-26

Summary

Fatigue experiments have previously been performed on welded austenitic stainless steel piping components subjected to both constant and variable amplitude loads. The results are reported in *Evaluation of fatigue in austenitic stainless steel pipe components* – SSM 2015:38 and offer the opportunity to evaluate fatigue flaw tolerance assessments used in industry and based on a fracture mechanical approach implemented in ProSACC (version 2.1, rev 2). The current investigation aims at validation of the used flaw tolerance approaches by comparing experimental results obtained for the total fatigue life of the considered piping component and the computed fatigue life estimates. More specifically, the conservatism of the approach is evaluated and a sensitivity analysis is performed to determine to which extent the uncertainty of selected input parameters contributes to the variation in estimated fatigue life.

The study indicates that a standard flaw tolerance approach inspired on ASME yields extensive conservatism, implying that the propagation fatigue life at most represents 10% of the total fatigue life, whereas a best-estimate flaw tolerance approach presents a significant reduction of conservatism, which indicates that fatigue initiation represents a negligible contribution to the total fatigue life for the performed fatigue experiments. The estimated 90% prediction limits of the best-estimate approach show good agreement with the experimental results.

The different assessments contain some potential sources for non-conservatism, such as uncertainties or approximations of the actual local stress field near the weld joint or even application of LEFM to potentially short cracks. Overall conservatism of the fatigue flaw tolerance approach is however preserved by postulating relatively large initial flaws and conservative assumptions regarding the fatigue growth law and determination of the fatigue crack driving force, which ensures increased fatigue crack growth rates. The sensitivity analysis highlights that the variation in the estimated fatigue life is best reduced by limiting or controlling the variation of the load, which may be accomplished by means of accurate load measurement or monitoring programs. To a lesser extent the variation in the fatigue growth law parameters also contributes to the variation in the estimated fatigue life.

The results support the use of flaw tolerance approaches for demonstrating reliability of a component using fracture mechanics methods, although the selection of input data was observed to significantly affect the overall degree of conservatism for the obtained fatigue life estimate. The performed work has contributed to verification of flaw tolerance approaches used in industry, which will facilitate the choice of optimal and safe control intervals for components subjected to fatigue loads.

Sammanfattning

Utmattningsprov har utförts på svetsade austenitiska rostfria rör som utsattes för både konstant och variabel amplitud belastning. Resultaten redovisades i *Evaluation of fatigue in austenitic stainless steel pipe components* - SSM 2015: 38 och möjliggör en utvärdering av de brottmekaniska analyser som används inom industrin och som grundar sig på en brottmekanisk metodik implementerad i ProSACC (version 2.1, rev 2). Den aktuella studien syftar till att validera analyserna genom jämförelse av beräknade livslängder med experimentella för de betraktade rören. Metodens konservatism utvärderas och bidraget av osäkerheten i utvalda inparametrar till den totala variationen i beräknade livslängd bestäms med hjälp av en känslighetsanalys.

Studien visar att brottmekanisk analys enligt ASME medför omfattande konservatism. En analys i stället baserat på en best-estimate visar en betydande minskning av konservatismen och indikerar att utmattningsinitieringen utgör ett försumbart bidrag till den totala utmattningslivslängden för de utförda experimenten. Det uppskattade 90% prediktionsintervallet för best-estimate analysen visar god överensstämmelse med de experimentella resultaten.

De genomförda analyserna enligt ASME uppvisar övergripande konservatism, trots osäkerheter kring det lokala spänningsfältet vid svetsfogen eller tillämpning av LEFM till potentiellt korta sprickor. Konservatism säkerställts genom att postulera relativt stora initiala defekter och konservativa antaganden för tillväxtlagen och skademekanismens drivkraft. Känslighetsanalysen belyser att variationen i beräknad livslängd minskas mest genom att kontrollera lastens variation, vilket kan åstadkommas med hjälp av noggrann lastmätning eller övervakningsprogram. I mindre utsträckning bidrar också variationen i tillväxtlagens parametrar till variationen i beräknad livslängd.

Resultaten stöder användning av brottmekanik för att visa tillförlitlighet hos en komponent, även om valet av indata påverkar nivån på konservatism i de uppskattade utmattningslivslängder. Studien har bidragit till verifiering av de skadetålighetsanalyser som används inom industrin och därmed underlättar valet av optimala och säkra kontrollintervall för komponenter som utsätts för utmattningslaster.

Contents 2016:27

1 Conclusive Summary

The current study presents a numerical investigation of fatigue flaw tolerance approaches based on fracture mechanical analyses, which are used to estimate fatigue life and determine service or inspection intervals for components. The investigation compared estimates of fatigue life for a welded austenitic stainless steel piping component computed using ProSACC (version 2.1 rev 2) with available experimental results. The numerical analyses considered fatigue flaw tolerance assessments of both internal and external fatigue cracks with a standard conservative approach inspired on ASME and a best-estimate approach. A parametric analysis using Variation Mode and Effect Analysis (VMEA) was also performed based on the best-estimate approach. The current study resulted in the following main findings:

- The conservative ASME inspired fatigue flaw tolerance approach yields extensive conservatism.
- The best-estimate flaw tolerance approach presents significantly reduced conservatism.
- The results of the best-estimate flaw tolerance approach imply a negligible contribution of fatigue initiation to the total fatigue life.
- The studied approaches contained potential sources of non-conservatism related to the assumed load description and applicability of LEFM.
- Overall conservatism of the fatigue flaw tolerance approach is preserved by means of conservative flaw geometry, material, load and fatigue growth assumptions.
- Variation of selected input data covering initial flaw geometry, growth law and load description induced relatively large variability of the estimated fatigue life.
- The VMEA indicated that the extent of the variability in the estimated fatigue life is primarily due to the variation or uncertainty in load.
- Load measurement or monitoring programs allowing for accurate load description enable to significantly reduce the variability in the estimated fatigue life.
- The estimated 90% predictions limits for the best-estimate flaw tolerance approach contained the experimental results.

The results support the use of flaw tolerance approaches for demonstrating reliability of a component using fracture mechanics methods, although the choice of input data is shown to strongly affect the overall degree of conservatism for the obtained fatigue life estimate. The performed work has contributed to verification of flaw tolerance approaches used in industry, which will facilitate the choice of optimal and safe control intervals for components subjected to fatigue loads.

2 Nomenclature

a	Crack depth
A	Cross-sectional area
c	Sensitivity coefficient
C	Fatigue growth law factor (Paris law)
C_0	Modified fatigue growth law factor to avoid accounting for crack closure effects
d_g	Average grain size diameter
E	Young's modulus
f	Transfer function used in sensitivity analysis
F	Normalized through-thickness evolvement of stress concentration factor
H	Geometry function in stress intensity factor formulation
$\mathcal{H}$	Integral included in expression of η
i,j	Dummy indices
I	Area moment of inertia of the cross-section
K	Stress intensity factor
K_t	Stress concentration factor
l	Crack length
L	Moment arm
m	Fatigue growth law exponent (Paris law)
n	Total number of (strain) cycles in a load sequence
N	Fatigue life, Total number of cycles (simulated or experimental)
N^{exp}	Total number of cycles (from fatigue experiments)
N^i	Total number of cycles consumed by fatigue crack initiation
N^p	Total number of cycles consumed by fatigue crack propagation
r	Radial coordinate of cross-sectional polar coordinate system
r_{pc}	Cyclic plastic zone radius
R	Load ratio
R_C	Ratio of fatigue growth law factors C
$R_{\mathcal{H}}$	Ratio of integrals $\mathcal{H}$
R_i	Inner radius of piping component
R_η	Ratio of Basquin equation factors η
R_σ	Stress ratio
s	Standard deviation
t	Wall thickness of piping component
u	Local radial coordinate with origin at fatigue crack initiation position
w	Coefficient of variation
x	Variable in sensitivity analysis
α	Exponent in Basquin equation for experimental or total fatigue life
β	Exponent in Basquin equation for experimental or total fatigue life
γ	Ratio of bending and membrane stress
$\Delta\blacksquare$	Range or difference
ε	Strain
η	Factor in Basquin equation for fatigue life consumed by propagation
κ	Factor in Basquin equation for experimental or total fatigue life
λ	Ratio estimated propagation fatigue life and total experimental fatigue life
μ	Mean value
ν	Poisson's ratio
σ	Pseudo-stress
σ_{yc}	Cyclic yield strength

τ	Contribution to standard deviation of logarithmic fatigue life
φ	Angular coordinate of cross-sectional polar coordinate system
χ	Ratio m-norm and β-norm
$\blacksquare_{a}$	Amplitude
$\blacksquare_{init}$	Quantity related to fatigue crack initiation (position)
$\blacksquare_{max}$, $\max\blacksquare$	Maximum value
$\blacksquare_{min}$	Minimum value
$\blacksquare_{nom}$	Nominal value
$\blacksquare_{th}$	Threshold value
$\blacksquare'$	Quantity related to logarithmic variable
$\blacksquare^{0}$	Quantity related to $\varphi = 0$
$\blacksquare^{\varphi}$	Quantity including a φ-dependence or evaluated at φ.
$\|\|\blacksquare\|\|_m$	m-norm

3 Introduction

3.1 Background

Components in nuclear power plants (NPPs) are subjected to various service induced degradation mechanisms. Fatigue is one of these mechanisms. Components are dimensioned to resist fatigue loads during the design service life time, often set to 40 years, based on design by analysis procedures contained in ASME Boiler and Pressure Vessel Code, Section III [1]. The fatigue design procedure is based on the determination of cumulative fatigue usage factors (CUFs) in air for fatigue sensitive components using prescribed design fatigue curves available for different materials. Early versions of the design requirements did however not include the detrimental effect of light water reactor environments on fatigue resistance, which was remediated by the introduction of the environmental correction factor (Fen), as described in NUREG/CR-6909 [2]. This correction factor can for some components introduce very large penalties, which may result in an unacceptable total fatigue usage factor, although the component initially complied with the original fatigue design requirements omitting environmental effects.

Safe and reliable long term operation (LTO) of the plant has to be demonstrated when NPPs approach the end of their design service life time, and apply for extension or renewal of the operating license. This process includes amongst others the evaluation of fatigue resistance of components considering the extended life time. The required fatigue analyses are however again based on fatigue usage factors following ASME, Section III [1]. Conservative design loads may be replaced with the actual fatigue load history observed during service life of a component, but showing compliance with the requirements for all components may reveal to be challenging, due to inherent (excessive) conservatism in the basic fatigue design methods.

When fatigue usage limits are exceeded, an alternative approach to demonstrate reliability of a component may be based on flaw tolerance methods. Such analyses postulate a flaw of a given size in the component and investigate the growth of the flaw. The flaw tolerance approach allows estimation of a fatigue life or necessary service intervals. These methods are currently under development for ASME, Section III [3], but already exist in the non-mandatory Appendix L of ASME Boiler and Pressure Vessel Code, Section XI [4]. However this particular section of the ASME code applies to in-service inspection, with procedures which are intended for demonstrating fitness for service. The flaw tolerance approach for fatigue is a fracture mechanical approach, where the input typically consists of a postulated initial flaw, a fatigue load and a fatigue crack growth law. Such fracture mechanical analyses are implemented in different commercial software such as ProSACC (version 2.1 rev 2), which are used in the industry and at NPPs. The output of the fatigue fracture mechanical approach depends however significantly on the selection of appropriate input data and modelling assumptions. Large variability in the results may be expected when applying different flaw tolerance analyses to a same problem, as illustrated in the round-robin study presented in [3]. It is therefore of interest to validate a fatigue flaw tolerance approach with experimental results.

3.2 Performed Piping Component Fatigue Tests

The experimental study reported in [5] included 28 test specimens consisting of seamless TP 304 LE stainless steel pipes joined with a circumferential single v-joint butt weld, see Figure 1 (a). At the vicinity of the circumferential butt weld the nominal wall thickness (t) and inner radius (R_i) were estimated at respectively 3 mm and 24.6 mm. The welding joints were in as-welded condition, i.e. the weld capping was not removed. All of the 28 test specimens were verified and approved with a radiographic examination.

All specimens were fatigue tested at room temperature (20°C) and subjected to reversed bending loading with displacement control in a standard single axis servo-hydraulic testing machine. The nominal axial strain was recorded with a strain gage situated in the bending plane. The experimental set-up was based on a construction using custom-built fixtures, which introduced a predominant bending stress and a small membrane stress [5], see Figure 1 (b). The piping components were during fatigue testing pressurized with water at 70 bar. Fatigue failure was defined by leakage, i.e. when the internal pressure could no longer be sustained.

The performed study had particular focus on high cycle fatigue (HCF) and variable amplitude (VA) loading. The fatigue experiments included both constant amplitude (CA) fatigue tests and experiments with variable amplitude loading using one out of three different load spectra:

- a piping spectrum (VAP), based on characteristic piping loads,
- a Gaussian spectrum (GAP), based on the piping spectrum, and
- a two-level block spectrum (VA2).

Each type of loading was performed at different severities for the considered loading types, except for the VA2 loading where only one severity was considered.

(a) (b)

Figure 1 (a) Welded piping component with close-up view of the circumferential butt weld in as-welded condition. (b) Actual mounted test specimen in servo-hydraulic testing machine.

Table 1 Selected fatigue results for the performed fatigue tests.

Pipe ID	Load type	Severity(*)	N^{exp} [cycles]	max $\varepsilon_{a,nom}$ [%]	Radial initiation position	φ_{init} [°]
1	VAP	Medium	575000	0.171	outside	34
2	VAP	Low	2500000	0.126	inside	0
3	VAP	High	217000	0.203	outside	161
4	VAP	Peak	139000	0.288	outside	30
5	VAP	Low	2520000	0.124	inside	17
6	VAP	Medium	253000	0.173	outside	17
7	VAP	High	269000	0.207	outside	8
8	VAG	Medium	941000	0.136	inside	-15
9	VAG	Medium	1063624	0.140	outside	0
10	VAG	High	126350	0.185	outside	12
11	VAG	Low	3921275	0.101	inside	26
(†)13	VAG	Low	5133411	0.103	-	-
14	VAG	High	247441	0.180	outside	-21
15	CA	2.2	740735	0.085	inside	172
(†)16	CA	1.7	5269515	0.065	-	-
18	CA	1.95	1027847	0.074	inside	-148
19	CA	2.6	291260	0.099	outside	6
20	VA2	-	1131716	0.069	inside	8
21	VA2	-	4880396	0.069	inside	-31
(†)22	VA2	-	5024628	0.068	-	-
23	VA2	-	913856	0.069	inside	8
24	VA2	-	321904	0.069	inside	171
25	CA	2.8	105769	0.109	outside	8
26	CA	2.8	144230	0.115	outside	0
27	CA	1.8	1367448	0.073	outside	-149
28	CA	1.7	512749	0.065	inside	9
(†)29	CA	1.7	5000000	0.068	-	-
(†)30	CA	1.7	5000000	0.067	-	-

(*) The severity for the CA experiments corresponds to the prescribed displacement amplitude.

(†) Run-out experiment, where the number of cycles exceeded the run-out limit of 5 million cycles. The fatigue tests were stopped prior to leakage and no fatigue initiation position was identified or detected.

Selected fatigue results for the 28 considered specimens are summarized in Table 1, where the total number of applied load cycles (N^{exp}) and the maximum nominal strain amplitude in the applied load sequence (max $\varepsilon_{a,nom}$) are reported from [5]. The radial (inside/outside) and circumferential position (φ_{init}) of fatigue initiation are taken from [6]. The circumferential position corresponds to the angular coordinate of a cross-sectional centered cylindrical coordinate system. The position of the strain gage situated in the bending plane of the specimen corresponds to a circumferential angle equal to zero. Additional information about the test specimens, experimental set-up, testing procedure, load description and/or obtained results is presented in [5, 7, 6].

The experimental results were used to investigate the margins of the design fatigue curve for austenitic steel in [1]. The work reported in [5, 7] contributed with:

- increased understanding of the ASME margins by highlighting extensive conservatism in the ASME fatigue procedure.
- improved knowledge on fatigue in austenitic stainless steel components and the fundamental issue of transferability.
- the development of an experimental procedure for fatigue testing of a realistic component allowing for more realistic margins and component specific design curves.
- highlighting the importance of using realistic variable amplitude (VA) loading to obtain reliable design curves, as opposed to using constant amplitude (CA) testing.

Continued work included a fractographic examination [6], which revealed:

- fatigue initiation occurring in the vicinity of weld toes near the bending plane both on the inside and outside of the weld joint.
- multiple adjacent fatigue cracks for specimens having been subjected to large strain amplitudes.
- leakage being the result of wall penetration due to a single dominant fatigue crack, which occasionally had merged with adjacent quasi-coplanar fatigue cracks.
- two distinct fatigue failure mechanisms for the considered thin-walled welded piping component yielding different fatigue crack features.

The different achievements of the performed work aimed at improving control of potential fatigue risks in piping components.

3.3 Objectives

The current study focusses on fracture mechanical analyses in order to estimate fatigue life and determine service intervals for components, following a fatigue flaw tolerance approach. The investigation will be performed using ProSACC (version 2.1 rev 2) and will include:

- a standard conservative approach similar to Appendix L in ASME XI [4],
- a best-estimate analysis in combination with a sensitivity analysis.

Based on the findings reported in [6], both fatigue crack propagation initiated from the inside and outside will be studied. Estimated number of cycles to failure will be compared to the experimental outcome obtained for the studied welded austenitic stainless steel piping component in [5], which will allow an estimation of the number of cycles consumed by crack initiation and consecutive crack propagation. Conservatism of the considered fatigue flaw tolerance approaches will be investigated.

The current investigation aims in particular at:

- providing increased reliability in fracture mechanics methods for fatigue in welded austenitic steel,
- contributing to the verification of damage tolerance approaches used in industry,
- facilitating the choice of optimal and safe control intervals for components subjected to fatigue loads.

4 Problem Description

4.1 Geometry

The overall geometry of the piping component is given by the nominal wall thickness (t) and inner radius (R_i) determined for the considered test specimen. The fatigue flaw tolerance approaches assume an initial circumferential planar crack with semi-elliptical shape, defined by crack depth (a) and crack length (l). The crack depth represents the flaw size in the radial direction, i.e. through the wall thickness. The total crack size in the circumferential direction is given by l, following the parameter definitions in ProSACC (version 2.1 rev 2) [8]. Based on the findings in [6], both an internal (initiation from inside) and an external (initiation from outside) initial crack are investigated. The postulated initial semi-elliptical crack is assumed to present an aspect ratio a/l = 1/6, which is also in accordance with the proposed assessment procedure in [3].

The postulated initial flaw geometry differs between the standard and best-estimate approaches by assuming a different initial crack depth. For the standard approach inspired by ASME, conservatism is ensured by taking an extended initial crack depth. For the best-estimate analysis a smaller crack depth is selected. A certain degree of conservatism will nevertheless also be maintained in the best-estimate approach. The selected initial ratios a/t for each analysis are summarized in Table 2. A ratio a/t = 1/10, as suggested in [3], was considered not suitable for the current investigation given the small wall thickness of the considered piping component.

Table 2 Postulated initial flaw depths.

Analysis	Standard	Best-estimate
initial a/t	1/2	1/6
initial a [mm]	1.5	0.5

4.2 Material

The TP 304 LE austenitic stainless steel piping component has material properties at room temperature (RT), defined at 20 °C, given by a Young's modulus, E = 200 GPa, and a Poisson's ratio, ν = 0.3. The cyclic yield strength is assumed to be similar to 316 L stainless steel used in [9], i.e. σ_{yc} = 405 MPa.The used fatigue flaw tolerance approaches assume crack growth following a Paris law:

$$\frac{\mathrm{d}a}{\mathrm{d}N} = C\,\Delta K^m \qquad (1)$$

where the crack growth rate ($\mathrm{d}a/\mathrm{d}N$) is expressed in terms of the stress intensity factor range, $\Delta K = K_{max} - K_{min}$, and two material parameters: the growth law factor C and growth law exponent m. In the current investigation the growth law exponent (m) is assumed to be constant and equal to the value prescribed in ASME XI, C-8410 [4] for crack growth in air in austenitic steels, i.e. m = 3.3. The present study will namely focus on fatigue crack growth in air, although crack initiation from the inside of the piping component occurred in water. Given the test conditions, the effect of water on the fatigue crack growth rate is assumed to be small [6], and is therefore not considered in the current study. The assumed value of m is also in agreement with experimental findings from [10], where fatigue crack growth law exponents at room temperature are reported in the range 3 - 4.

Table 3 Assumed fatigue growth law factors for the performed flaw tolerance approaches.

Analysis	Standard	Best-estimate
C [mm/cycle]	$2.05\ 10^{-9}$	$6.80\ 10^{-10}$

The standard and best-estimate approaches differ by assuming a different growth law factor C, as presented in Table 3. The standard approach follows the fatigue growth law description stipulated in ASME XI, C-8410 [4], where the growth law factor for crack growth in air in austenitic steels a priori depends on temperature and load ratio $R = K_{min} / K_{max}$. The latter dependence is though only applied for positive load ratios. In the current investigation the temperature is however constant (20°C) and predominant reversed bending loads induce $R \leq 0$, giving the constant growth law factor in Table 3. The best-estimate approach will assume a less conservative or smaller constant growth law factor based on experimental results in [10]. The work performed in [10] includes the determination of fatigue crack growth rates at room temperature using specimens machined from a welded 304 austenitic stainless steel pipe and subjected to fatigue testing at $R = 0.1$.

Equation (1) is usually assumed valid for ΔK exceeding a constant threshold value, ΔK_{th}. In the current investigation fatigue crack growth will be modelled assuming $\Delta K_{th} = 0$. This assumption preserves conservatism, as even small load cycles can contribute to fatigue crack growth. Furthermore, it ensures the results to be unaffected by possible history or sequence effects occurring in VA fatigue loads.

4.3 Load

The fatigue cracks in the piping component are subjected to different load contributions affecting their growth. During fatigue testing the specimens were water pressurized with a constant internal pressure of 70 bar, affecting the mean load or load ratio R. The custom-built fixtures allowed furthermore to subject the specimens to a principal bending load. The bending moment prevailing between the fixtures is given by the alternating vertical force at the hydraulic testing machine and the moment arm L = 300 mm. The alternating vertical force also induced a minor membrane load in the test specimen. Both bending and membrane loads are alternating during testing of the piping components inducing the fatigue crack growth driving loads. During testing the nominal strain was recorded by means of a strain gage situated in the bending plane of the specimen [5].

5 Theory and Methods

5.1 Flaw tolerance approach

The flaw tolerance approach is performed using ProSACC (version 2.1 rev 2). Apart from a (crack) geometry definition and selection of a crack growth law description, ProSACC requires both a minimum and maximum local through-thickness stress distribution as input for the implemented fracture mechanical analysis. During calculations these stress profiles are in the current study approximated with a third order polynomial fit over the considered crack depth. Note that the implementation in ProSACC does not include variation of the stress field in the circumferential direction. Effects of stress variation in the circumferential direction on fatigue crack growth are therefore neglected.

5.1.1 Load model

A load model has been adopted to account for the different load contributions present during testing. It aims at providing the necessary minimum and maximum local through-thickness stress profiles present at the considered initiation position for a given nominal strain amplitude. The minimum and maximum local stress profiles are equivalently determined by the distributions of the local pseudo-stress amplitude σ_a and pseudo-stress ratio $R_\sigma = \sigma_{min} / \sigma_{max}$, which are defined by the current load model.

A cross-sectional centered polar coordinate system (r, φ) is introduced, where $\varphi = 0$ indicates the circumferential position of the strain gage, situated in the bending plane, see [5, 6] for more details. The stress fields will differ depending on the radial initiation position; hence a local coordinate u is introduced, which is function of r:

$$u = r - R_i \text{ , for a crack initiated from inside,} \quad (2)$$

$$u = R_i + t - r \text{ , for a crack initiated from outside.} \quad (3)$$

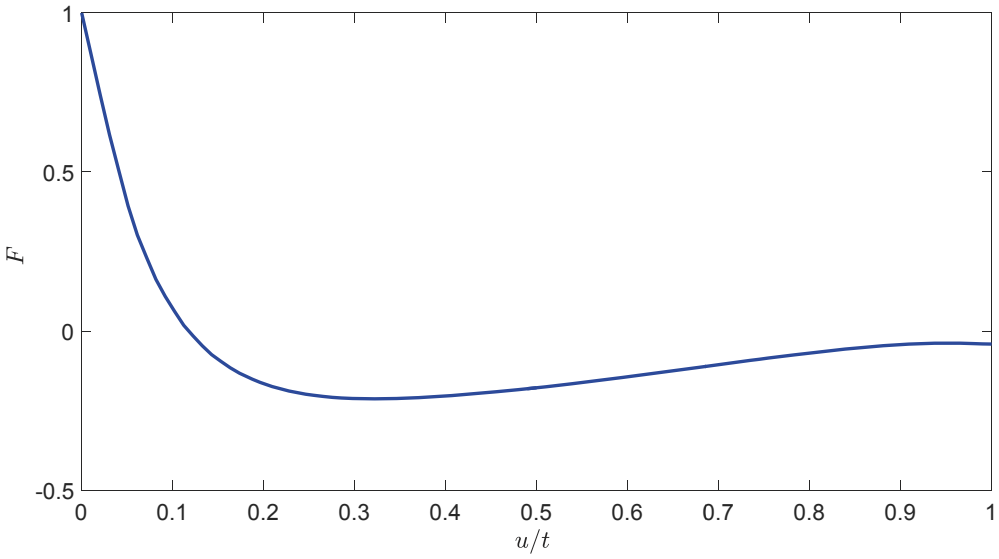

Figure 2 Normalized through-thickness evolvement of stress concentration due to the presence of a weld toe.

During fatigue testing nominal strains were recorded, which for the fatigue flaw tolerance approaches were transformed in a nominal linear elastic pseudo-stress by means of E. The transformation from nominal to local stress or strain is performed assuming a constant concentration factor K_t = 1.4 [5] and a through-thickness evolvement defined by means of a function F, illustrated in Figure 2. The normalized through-thickness evolvement of the stress concentration factor at a weld toe was computed using a finite element (FE) simulation similar to the one used for the estimation of K_t in [5]: the FE analysis assumed a weld geometry given by a cap height of 0.5 mm and weld toe radius of 1 mm. The mesh size was approximately 0.1 mm and the simulation was performed using ANSYS 14.5 [11]. K_t and F are assumed identical for cracks starting from inside and outside. The shape of F in Figure 2, indicates that the stress concentration mainly acts down to a depth of approximately 10% of the wall thickness, whereas a stress field close to the nominal stress field is expected to act over the remaining, major part of the wall thickness.

The predominant load is related to the alternating bending moment prevailing between the fixtures. The experimental set-up induces also a minor alternating membrane stress, which was found affecting localization of fatigue crack initiation, see [6]. The ratio of bending and membrane stress is given by the dimensionless factor $\gamma = A\ L\ (R_i + t)\ /\ I$, where A and I represent respectively the cross-sectional area and the area moment of inertia of the cross-section for the studied piping component. For the considered pipe geometry and experimental set-up, γ = 24.2, which highlights the predominance of the bending stress. The local pseudo-stress amplitude is a function of the polar coordinates, and is assumed to be given by the following expression:

$$\sigma_a(r,\varphi) = [(K_t - 1)\,F(r) + 1]\left[\left(\frac{1}{1+\gamma}\right) + \left(\frac{1}{1+{}^{1}/_{\gamma}}\right)\frac{r}{R_i + t}\right] E\,\varepsilon_{a,nom}^{\varphi} \qquad (4)$$

where the first bracket accounts for the transfer from nominal to local stress. The second bracket considers the linear r dependency of the nominal pseudo-stress. Considering the negligible contribution of the membrane stress, the φ dependency was approximated by factorization to be included in the expression a nominal strain amplitude defined in terms of φ and the nominal strain amplitude at the strain gage $\epsilon_{a,nom}^{0}$, i.e. at φ = 0 (and $r = R_i + t$):

$$\varepsilon_{a,nom}^{\varphi} = |\cos\varphi|\,\varepsilon_{a,nom}^{0} \qquad (5)$$

For a crack initiated at $\varphi = \varphi_{init}$, the local through-thickness pseudo-stress amplitude distribution is then given by $\sigma_a(r, \varphi_{init})$. The developed load model is intended for use with small angular coordinates, i.e with φ_{init} relatively close to 0, which was shown to be the most probable position for crack initiation [6]. At the secondary most probable initiation position, i.e. in the vicinity of φ_{init} = 180°, the model somewhat over-estimates the local stress amplitude, as it assumes membrane stress to act in phase with bending stress. At these locations, this minor over-estimation does however ensure conservatism of the performed flaw tolerance assessments. The through-thickness distribution of the normalized stress amplitude is illustrated in Figure 3 (a).

The constant internal pressure induces a local mean stress distribution near the weld, which gives the pseudo-stress ratio distribution illustrated in Figure 3 (b) for $\varepsilon_{a,nom}^{\varphi}$ = 0.1%. Considering lower nominal strain amplitudes yields an increase in pseudo-stress ratio, which does however remain negative for the performed experiments. The mean load distribution is independent of the circumferential position, but differs between considered radial crack initiation positions. For cracks

that started from inside the internal pressure gives an additional contribution as a constant crack face pressure. The mean load is expected to be affected by the through-thickness weld residual stress distribution, which was however not included in the current investigation. Similarly as in [3], the weld residual stress is thus assumed to be zero.

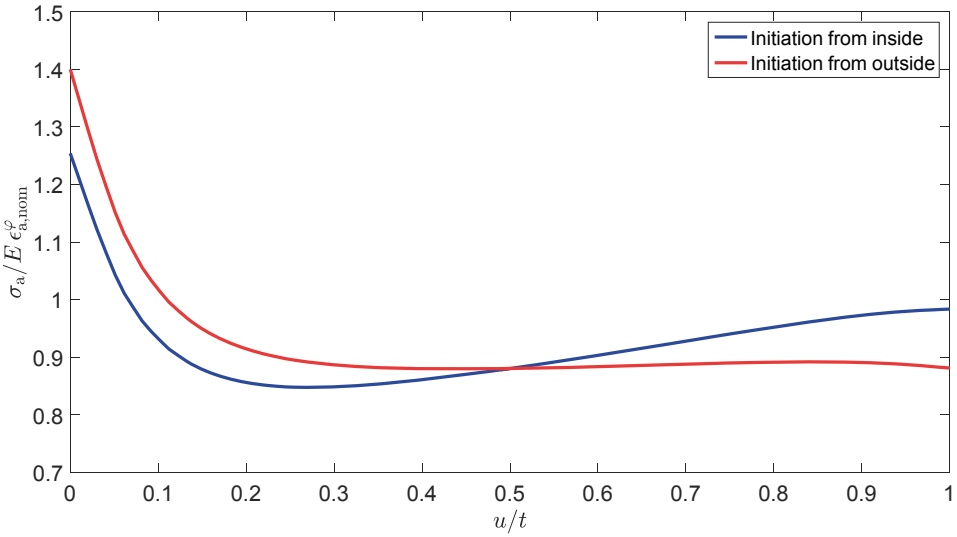

(a)

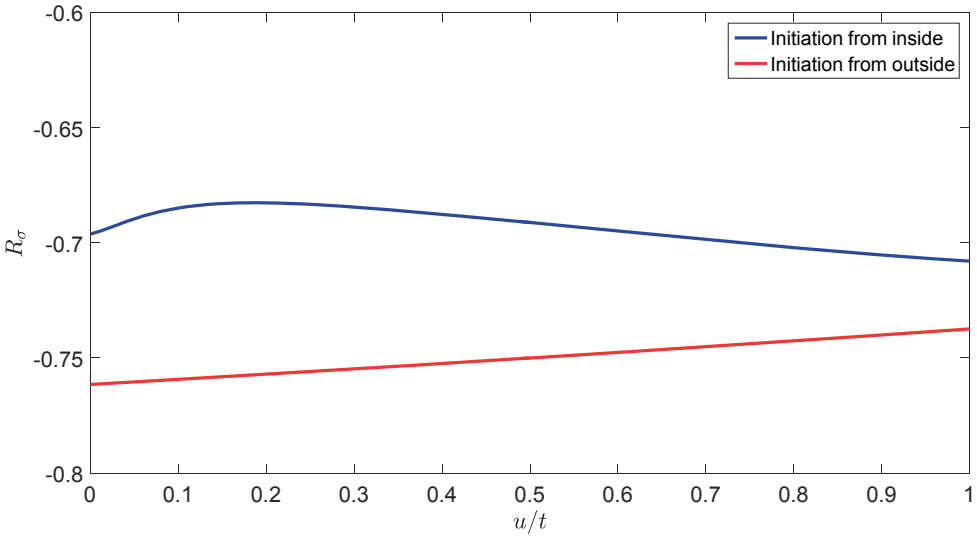

(b)

Figure 3 Through-thickness evolvement of (a) normalized pseudo-stress amplitude and (b) pseudo-stress ratio for a nominal strain amplitude at the initiation position of 0.1%.

5.1.2 Equivalent strain amplitude measure

The load model in Equation (4) requires a scalar nominal strain amplitude, which is directly available for CA tests, but not for VA tests. For fatigue tests using VA loads, an equivalent strain amplitude measure needs therefore to be defined. For the current fracture mechanical approach an equivalent strain amplitude measure based on the fatigue growth law exponent m is selected. The equivalent measure for a load sequence consisting of n strain cycles with amplitude $\varepsilon_{a,i}$, is then expressed in terms of the m-norm of the strain amplitudes.

$$\|\varepsilon_a\|_m = \left(\frac{1}{n}\sum_i^n \varepsilon_{a,i}^m\right)^{1/m} \tag{6}$$

This equivalent strain amplitude measure differs in general from the β-norm strain defined in [5], as $m \neq \beta = 4.6$. For a given type of load spectrum the ratio of the m-norm and β-norm, denoted χ, will however be constant. In absence of a threshold value, the magnitude of the considered load spectrum will not affect this ratio. The ratios for the considered load types are given in Table 4.

Table 4 Ratio of m-norm and β-norm strains from [5] for different load types.

Load type	VAP	VAG	CA	VA2
χ	0.842	0.881	1.000	0.974

Table 5 presents different nominal strain measures for the performed fatigue tests. The m-norm strain at $\varphi = 0$ is denoted $\left\|\varepsilon_{a,nom}^0\right\|_m$ and is computed using the relevant χ in Table 4 and the β-norm strain available in [5]. The m-norm strain at the initiation position tabulated in Table 1, is denoted $\left\|\varepsilon_{a,nom}^{\varphi_{init}}\right\|_m$ and is determined using Equation (5). This equivalent strain measure is by definition smaller the m-norm strain at $\varphi = 0$, but no large differences are observed, as the absolute value of the cosine of φ_{init} is relatively close to unity. For run-out experiments, a circumferential initiation position is not available. It was then assumed to be given by the most probable location for fatigue crack initiation, i.e. $\varphi_{init} = 0$ [6].

Table 5 Different nominal strain measures for the performed fatigue tests.

Pipe ID	Load type	Severity(*)	$\max \varepsilon_{a,nom}$ [%]	$\left\|\varepsilon_{a,nom}^{0}\right\|_m$ [%]	$\left\|\varepsilon_{a,nom}^{\varphi_{init}}\right\|_m$ [%]
1	VAP	Medium	0.171	0.061	0.051
2	VAP	Low	0.126	0.045	0.045
3	VAP	High	0.203	0.073	0.069
4	VAP	Peak	0.288	0.096	0.083
5	VAP	Low	0.124	0.044	0.042
6	VAP	Medium	0.173	0.060	0.057
7	VAP	High	0.207	0.072	0.072
8	VAG	Medium	0.136	0.054	0.052
9	VAG	Medium	0.140	0.057	0.057
10	VAG	High	0.185	0.073	0.071
11	VAG	Low	0.101	0.042	0.038
(†)13	VAG	Low	0.103	0.041	0.041
14	VAG	High	0.180	0.065	0.061
15	CA	2.2	0.085	0.085	0.084
(†)16	CA	1.7	0.065	0.065	0.065
18	CA	1.95	0.074	0.074	0.063
19	CA	2.6	0.099	0.099	0.098
20	VA2	-	0.069	0.059	0.059
21	VA2	-	0.069	0.059	0.051
(†)22	VA2	-	0.068	0.059	0.059
23	VA2	-	0.069	0.059	0.059
24	VA2	-	0.069	0.059	0.059
25	CA	2.8	0.109	0.109	0.108
26	CA	2.8	0.115	0.115	0.115
27	CA	1.8	0.073	0.073	0.062
28	CA	1.7	0.065	0.065	0.064
(†)29	CA	1.7	0.068	0.068	0.068
(†)30	CA	1.7	0.067	0.067	0.067

(*) The severity for the CA experiments corresponds to the prescribed displacement amplitude.

(†) Run-out experiment, where the number of cycles exceeded the run-out limit of 5 million cycles: $\varphi_{init} = 0$ is assumed.

5.1.3 Propagation fatigue life

The number of cycles to failure consumed by fatigue crack propagation is obtained by integration of Equation (1), where the stress intensity factor range can be expressed in terms of the strain amplitude and a geometry function H characteristic for a given crack geometry:

$$\Delta K = \varepsilon_{\mathrm{a}}\, H \tag{7}$$

In the current investigation two semi-elliptical crack configurations (internal and external) are considered, which will consequently have different geometry functions H. Furthermore will these functions depend on the flaw size, i.e. a and l. Integration of Equation (1), considering Equation (7), yields

$$N = [C^{-1}\,\mathcal{H}]\;{\varepsilon_{\mathrm{a}}}^{-m} = \eta\;{\varepsilon_{\mathrm{a}}}^{-m} \tag{8}$$

which is a Basquin type equation with factor η and an exponent giving by the fatigue crack growth law (Paris law) exponent m. The factor η is given by $\mathcal{H}/C$, where $\mathcal{H}$ is an integral with the initial and final crack depth as integration limits and H^m as integrand. The expression of N in Equation (8) can be generalized to be applicable to VA load by summation of the different strain amplitude contributions:

$$N = [C^{-1}\,\mathcal{H}]\;(\|\varepsilon_{\mathrm{a}}\|_m)^{-m} = \eta\;(\|\varepsilon_{\mathrm{a}}\|_m)^{-m} \tag{9}$$

The expression includes the m-norm of the strain amplitude defined in Equation (6). The m-norm strain can thus be interpreted as the equivalent CA strain amplitude yielding identical fatigue life (number of cycles of propagation) as the original VA load sequence, for a given final crack size. The derivation assumes sequence or history effects to be negligible. Such effects are indeed not accounted for due to the assumption of $\Delta K_{\mathrm{th}} = 0$.

The stress intensity factor formulations implemented in ProSACC are based on tabulated solutions, see [8], which present a range of applicability $a/t \leq 0.8$. Hence, ProSACC will only allow computation of the number of cycles corresponding to propagation from the initial crack depth up till $a = 0.8\,t$. It will be assumed that $N_{a=0.8t}$ is a conservative estimate of the number of cycles to leakage starting from a postulated initial flaw size. Continued propagation of the fatigue crack up to wall penetration, i.e. $a = t$, and leakage, is namely expected to occur with significantly increased fatigue crack growth rates. Additionally is linear elastic fracture mechanics (LEFM) expected to be no longer applicable during the final stages of fatigue crack growth up to wall penetration.

For given fatigue growth law parameters and final crack depth, Equation (9) indicates that $\eta = N(\|\varepsilon_{\mathrm{a}}\|_m)^m$ is constant. This observation avoids performing ProSACC simulations for each specimen separately, as only one simulation suffices to determine the factor η. The number of cycles to failure, N, for each specimen is then estimated by means of Equation (9) with $\|\varepsilon_{\mathrm{a}}\|_m = \left\|\varepsilon_{\mathrm{a,nom}}^{\varphi_{\mathrm{init}}}\right\|_m$, tabulated in Table 5.

5.1.4 Crack closure effects

In the current study, conservatism of the considered flaw tolerance approaches is ensured by not considering crack closure effects on fatigue life, as crack closure tends to reduce the crack growth driving force.

For the standard flaw tolerance approach, the fatigue growth law implementation in ProSACC is based on the formulation in ASME XI [4], where the total extent of the stress intensity factor range is used, even for $R \leq 0$:

$$\Delta K = K_{\max} - K_{\min} = K_{\max}\,(1 - R) \tag{10}$$

Consequently, crack closure effects are not considered in the definition of ΔK.

The best-estimate analysis is performed using the 'fatigue growth law defined by coefficients' implemented in ProSACC. This implementation uses however an effective stress intensity factor range to account for crack closure effects, which for $R \leq 0$ is given by

$$\Delta K = K_{\max} \tag{11}$$

In order to deal with crack closure effects in a similar way as the standard approach and avoid reduced fatigue crack growth rates, the fatigue growth law factor was modified considering Equation (1) and comparing Equations (10) and (11):

$$C_0 = C\,(1 - R)^m \approx 6\,C = \ 4.08\ 10^{-9} \tag{12}$$

The modified fatigue growth law factor will be used as input in ProSACC and is assumed common for both investigated crack geometries. The multiplicative factor 6 is derived by approximating the load ratio R with the overall mean value of the pseudo-stress ratio in Figure 3 (b), considering both crack geometries, which resulted in approximately -0.72. This approximation was enabled as R_σ in Figure 3 (b) is relatively constant through the thickness.

The considered flaw tolerance approaches initially consider crack closure effects differently, which is remediated by modifying the input for the best-estimate approach, i.e. using C_0 from Equation (12) instead of C in Table 3.

5.2 Comparison between experiments and fracture mechanical fatigue assessments

The experimental fatigue life, N^{exp}, reported in Table 1, from [5], corresponds to the total fatigue life of the investigated piping component and can be subdivided in two separate contributions:

$$N^{\exp} = N^{i} + N^{p} \tag{13}$$

where the first term, N^i, refers to the number of cycles necessary for fatigue initiation to occur, and the second term, N^p, represents the fatigue life consumed during propagation of the fatigue crack up till leakage of the piping component. Equation (13) allows thus to examine the subdivision of total fatigue life in initiation and propagation.

5.2.1 Fatigue life consumed by propagation, N^p

The fracture mechanical fatigue analyses performed during the current investigation are based on LEFM and aim at estimating Np, using the Basquin relation in Equation (9). The estimate does however not include propagation up to the postulated initial flaw and final propagation for a > 0.8t. The latter contribution is assumed negligible compared to the total fatigue life, whereas the former contribution can be transferred to Ni. Early fatigue crack propagation is though commonly also neglected due to the significantly increased crack growth rates observed for short or small fatigue cracks, when compared to the growth rates of long or large fatigue cracks [12]. Furthermore is LEFM expected to be not applicable for short or small flaws.

5.2.2 Experimental or total fatigue life, N^{exp}

In [5], N^{exp} was fitted with a Basquin relation using the VAP and VAG data points, yielding,

$$N^{\exp} = \alpha\left(\|\varepsilon_a\|_\beta\right)^{-\beta} \tag{14}$$

with α =2.89 and β = 4.6. Additionally the coefficient of variation of N^{exp} was estimated to be 0.42. It can be noted in Table 4 that the relative difference between the χ ratios for VAP and VAG is less than 5%. It can thus be assumed that the VAP and VAG data points have a common χ ratio equal to their weighted mean value, i.e. χ = 0.860. Equation (14) can then be reformulated in terms of the m-norm strain amplitude, allowing direct comparison with N^p given in Equation (9):

$$N^{\exp} = \alpha\left(\frac{\|\varepsilon_a\|_m}{\chi}\right)^{-\beta} = \left[\alpha\,\chi^{\beta}\right]\left(\|\varepsilon_a\|_m\right)^{-\beta} = \kappa\left(\|\varepsilon_a\|_m\right)^{-\beta} \tag{15}$$

Through identification, the factor κ is then estimated to be 1.44. Comparison of experimental results with N^p is of importance in the investigation of the margins of a fatigue flaw tolerance approach and allows the study of the conservatism included in the used approach.

5.2.3 Sensitivity analysis applied to propagation fatigue life

The standard fatigue flaw tolerance approach using recommendations from ASME is expected to yield a conservative estimate of the propagation fatigue life. However no information is available about the variation of the result due to uncertainty in the input parameters. The sensitivity analysis based on a best-estimate analysis, aims at studying the variation in estimated fatigue life and investigating which properties of the fracture mechanical assessment have a dominant effect on the estimated fatigue life variation. This parametric procedure is known as Variation Mode and Effect Analysis (VMEA) [13].

The procedure is based on a linearization of a transfer function. To reduce effects of non-linearities, the sensitivity analysis considers the logarithmic fatigue life. For the current investigation four assumed independent logarithmic stochastic variables, $\ln x_j$, are considered:

$$\ln N = f(\ln(\|\varepsilon_a\|_m), \ln C, \ln a, \ln l) \tag{16}$$

where f denotes the transfer function and the variables x_j cover the effects on fatigue life of load ($\|\varepsilon_a\|_m$), material (C) and initial crack geometry (a and l). The effects of other parameters such as for instance the nominal pipe geometry dimensions or the fatigue growth law exponent have not been directly included in the current study. A more explicit expression of the transfer function is obtained by taking the natural logarithm of Equation (9) yielding,

$$\ln N = -m \ln(\|\varepsilon_a\|_m) - \ln C + \ln(\mathcal{H}(\ln a, \ln l)) \tag{17}$$

The expected values (μ') and standard deviations (s') of the selected logarithmic variables are considered known. They can namely be expressed as follows for a given variable x_j:

$$\mu'_j = \mu_{\ln x_j} \approx \ln \mu_{x_j} = \ln \mu_j \tag{18}$$

$$s'_j = s_{\ln x_j} \approx \frac{s_{x_j}}{\mu_{x_j}} = \frac{s_j}{\mu_j} = w_j = w_{x_j} \tag{19}$$

where w_j denoted the coefficient of variation of variable x_j.

Under the assumption that the input variables are independent, the standard deviation of the logarithmic fatigue life is approximated by means of the Gauss approximation formula:

$$s_{\ln N} = s'_N \approx \sqrt{\sum_{j=1}^{4} c_j^2 s_{\ln x_j}^2} \approx \sqrt{\sum_{j=1}^{4} c_j^2 w_j^2} = \sqrt{\sum_{j=1}^{4} \tau_j^2} \tag{20}$$

where c_j denotes the sensitivity coefficient belonging to $\ln x_j$. Equation (20) yields thus an estimation of the coefficient of variation of the propagation fatigue life, i.e. w_N. The sensitivity coefficients are the partial derivatives of the transfer function with respect to the input variables taken around the expected values of the input values, which for a given variable x_j gives:

$$c_j = c_{\ln x_j} = \left.\frac{\partial f}{\partial(\ln x_j)}\right|_{\mu'} \tag{21}$$

Considering Equation (17), analytical expressions of these sensitivity coefficients can be derived for the load or equivalent nominal strain amplitude and the fatigue crack growth law factor *C*:

$$c_{\ln(\|\varepsilon_a\|_m)} = -m \tag{22}$$

$$c_{\ln C} = -1 \tag{23}$$

However for the two remaining variables related to the initial crack geometry no analytical solutions are directly available. The sensitivity coefficients are then estimated numerically by a central difference approximation using ProSACC.

Knowing the standard deviation of the logarithmic fatigue life by means of Equation (20), allows the determination of prediction limits. The 90% prediction limits will be determined assuming a normal distribution of the logarithmic fatigue life, and aims at illustrating the variation in estimated fatigue life due to variation in selected input parameters for the best-estimate flaw tolerance approach.

6 Results

6.1 Estimate of expected propagation fatigue life

The mean fatigue life consumed by propagation, N^p, is estimated using Equation (9). As the exponent m is kept constant, only the factor η will differ between considered flaw tolerance approaches and crack geometries. Table 6 summarizes the results for the performed simulations with a nominal strain amplitude of 0.01%. Note that the reported values are intended to be used in conjunction with strain amplitudes expressed in %. A larger factor η indicates longer fatigue life or slower fatigue crack growth. The results in Table 6 indicate that fatigue crack growth starting from an internal flaw is slower when compared to the external flaw, which is explained by the difference in load, see Figure 3 (a). The differences between flaw tolerance approaches are related to the differences in fatigue growth law factor C, see Table 3, and the extent of simulated fatigue growth, as different initial flaw sizes are postulated. The standard and best-estimate analyses corresponded respectively to 0.9 and 1.9 mm of simulated fatigue crack growth. The best-estimate approach used a lower fatigue growth law factor and smaller initial flaw size, than the standard conservative approach based on ASME XI [4]. These differences explain the larger number of cycles necessary to propagate through the wall thickness of the piping component using the best-estimate approach.

The relative effect on expected fatigue life of the differences in C and postulated initial flaw size between performed flaw tolerance assessments, are estimated by considering the difference in logarithmic fatigue life (to obtain additive contributions) and the definition of η introduced in (8):

$$\Delta(\ln N) = \ln R_\eta = \ln \frac{R_{\mathcal{H}}}{R_C} = -\ln R_C + \ln R_{\mathcal{H}} \qquad (24)$$

where R_η, R_C and $R_{\mathcal{H}}$ refer respectively to the ratios of factor η, fatigue growth law factor C and the initial flaw size dependent integral $\mathcal{H}$. Based on Table 3, R_C = 0.33. The relative contribution of C to the difference in logarithmic fatigue life is then given by - ln R_C / ln R_η, whereas the complementary relative contribution of the initial flaw size is computed as 1+ ln R_C / ln R_η. The relative contributions are computed in Table 6 for both considered crack geometries. The results indicate that the difference in fatigue growth law factor contributes to approximately 1/3 of the difference in expected propagation fatigue life, whereas the remaining 2/3 is due the difference in postulated initial flaw size. The latter contribution plays thus a predominant role.

Table 6 Estimate of η factor in Equation (9), for different studied flaw tolerance approaches and crack geometries. The relative contributions of C and the initial flaw size to the change in ln(η) are included.

Crack geometry or initiation location	η		R_η	Relative contributions	
				C	initial a and l
	Flaw tolerance assessment			$\frac{-\ln R_C}{\ln R_\eta}$	$\frac{\ln R_{\mathcal{H}}}{\ln R_\eta} = 1 + \frac{\ln R_C}{\ln R_\eta}$
	Standard	Best-estimate			
Internal	2.45	64.7	26.41	34%	66%
External	1.61	52.5	32.6	32%	68%

Figure 4 illustrates the different estimates of fatigue life and related prediction limits for both the conservative standard and best-estimate approaches obtained for the two investigated crack geometries. The estimate of the mean total fatigue life based on experimental results (N^{exp} - mean) is defined by Equation (15) and represented with a solid black curve. The dashed black curve (N^{exp} - 90%) corresponds to the lower 90% prediction limit or design curve derived in [5]. Experimental data points relevant for the considered crack geometry are included in Figure 4 using $\left\|\varepsilon_{a,nom}^{\varphi_{init}}\right\|_m$ in Table 5 as equivalent strain measure. The different symbols used for the experimental data points refer to the different load types. The mean expected fatigue life consumed by propagation obtained with the standard approach (N^p - ASME) and best-estimate approach (N^p - VMEA - mean), are respectively represented with a magenta and cyan solid curve. These mean curves are defined by Equation (9) and the η factors in Table 6.

A first difference between the mean curves for N^{exp} and N^p is the difference in slope, which is due to the different exponents of the Basquin equations, i.e. $m \neq \beta$. The estimate of N^p using the standard approach inspired on ASME XI [4] is always situated below the fitted estimate of N^{exp}, for the considered equivalent strain amplitudes. This observation is valid for both considered crack geometries and illustrates the extensive conservatism of the standard approach. Using a flaw tolerance approach based on the best-estimate approach preserves conservatism for equivalent strain amplitude less than 0.05 %. For the smaller equivalent strain amplitudes a significant reduction of conservatism is obtained. For larger equivalent strain amplitudes the mean estimate of propagation fatigue life exceeds the fitted estimate of N^{exp}, resulting in non-conservatism. It can however be noted that the extent of conservatism for the best-estimate approach will strongly depend on the slope of the mean curve, i.e on the fatigue growth law exponent m which was assumed equal to the one of the standard approach. Larger exponents are expected to increase conservatism of the best-estimate approach.

When the N^p estimates are assumed to represent the total number of cycles of fatigue life consumed by propagation, then one can compute the ratio $\lambda = N^p / N^{exp}$, for the different crack geometries and flaw tolerance approaches, see Figure 5. The ratio λ indicates then the portion of the total fatigue life consumed by propagation, whereas 1- λ would inform about the portion of the total fatigue life consumed by initiation.

For the standard approach, the total fatigue life consumed by actual crack propagation is less than 10% for the smaller equivalent strain amplitudes, whereas it is approximately less than 20% for the larger equivalent strain amplitudes. For the smallest considered equivalent strain amplitudes the standard flaw tolerance approach predicts that almost the entire total fatigue life is consumed by fatigue crack initiation. For the best-estimate approach, λ is larger as it predicts a larger portion of the fatigue life to be consumed by propagation of the flaw. For equivalent strain amplitudes exceeding approximately 0.05 %, λ approaches unity, which can be interpreted as a negligible contribution of fatigue crack initiation to the total fatigue life. An increase in λ is observed for increasing equivalent strain amplitudes, i.e. fatigue crack initiation represents a smaller part of the total fatigue life when larger loads are applied. These results indicate that a larger portion of the total fatigue life is consumed by initiation for the smaller equivalent strain amplitudes than for the larger ones.

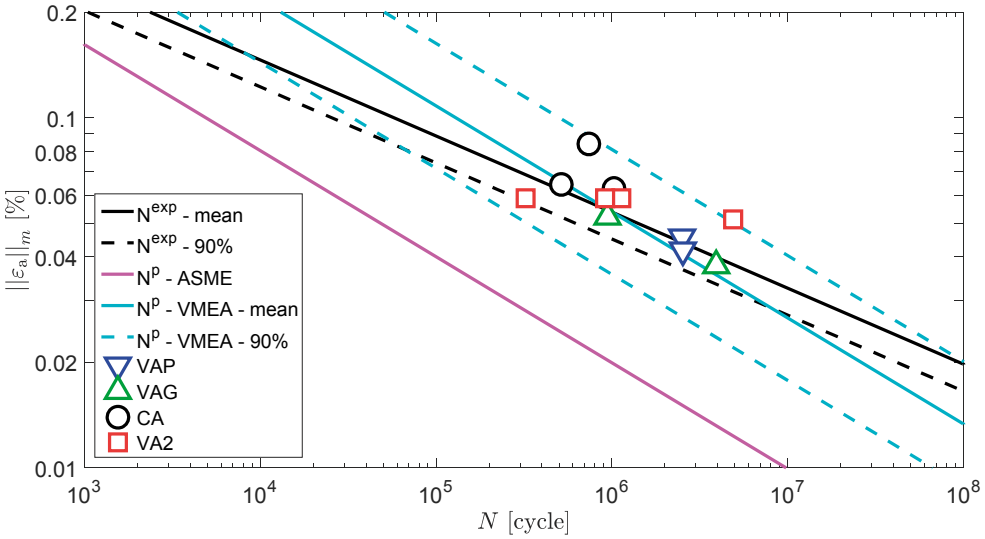

(a)

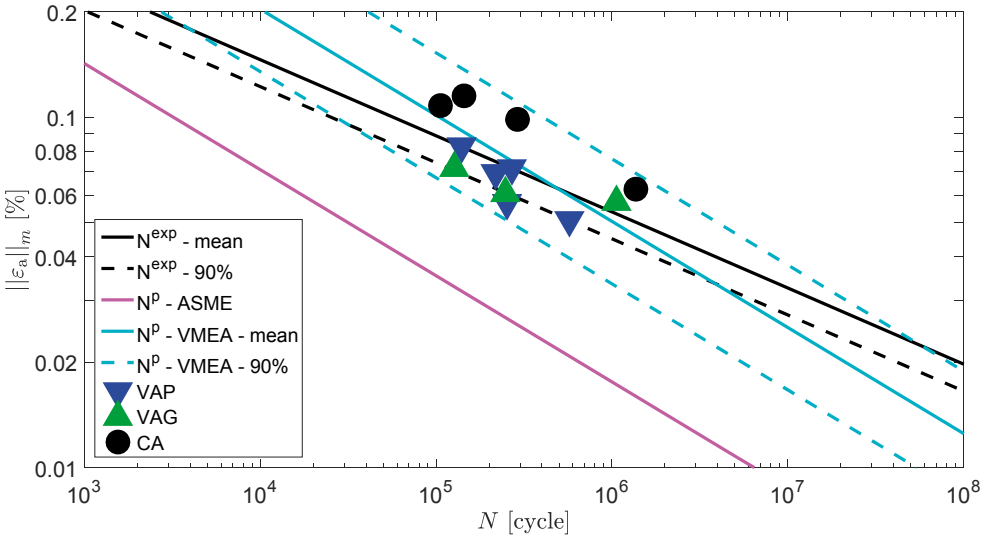

(b)

Figure 4 Equivalent strain amplitude *vs* number of cycles for (a) an internal fatigue flaw and (b) an external fatigue flaw.

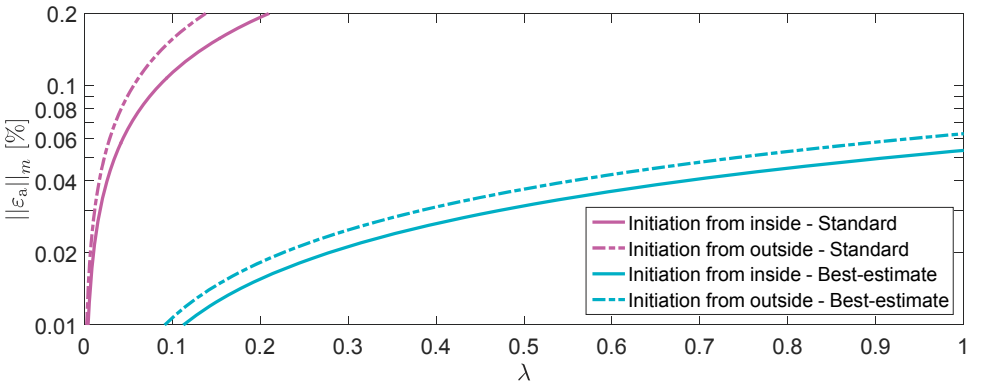

Figure 5 Equivalent strain amplitude *vs* portion of total fatigue life consumed by propagation.

6.2 Sensitivity analysis

The best-estimate approach was also used as basis for a sensitivity analysis using VMEA, which resulted in an estimate of the standard deviation of the logarithmic propagation fatigue life. The estimate is based on the consideration of four variables and their respective coefficients of variation. Table 7 lists the contributions of each variable to the total variance of the logarithmic propagation fatigue life for the two considered crack geometries. The results for each considered crack geometry differ by the sensitivity coefficients for a and l, which were determined numerically. All sensitivity coefficients of the considered variables are negative, which indicates that an increase of the variable will result in a reduction of the fatigue life. The equivalent strain amplitude presents the largest sensitivity coefficient, which is directly related to the magnitude of the fatigue growth law exponent.

Comparison of τ_j^2 in Table 7 for each variable allows estimating relative contributions of the considered variables to the total variance of the logarithmic propagation fatigue life, see Equation (20). The results indicate that the crack size dimensions contribute with about 5%, whereas the fatigue growth law factor and the equivalent strain amplitude present considerably larger contributions of respectively 30 and 65%. Consequently the variation in equivalent strain amplitude will give the largest contribution to the variation of the estimated propagation fatigue life. For the current study, based on controlled fatigue experiments, the coefficient of variation for the equivalent strain amplitude was assumed to be 0.2. An increase of this coefficient of variation in applications with more uncertainty in the applied load will induce a significantly increased w_N, which is due to the relatively large sensitivity coefficient. In such a case, the relative contribution of the load to the total variance of the logarithmic propagation fatigue life will rapidly become predominant. Consequently, accurate load description is of importance in a flaw tolerance approach to reduce the variability of the estimated fatigue life.

Although the sensitivity coefficients for the fatigue flaw size variables differ between the considered crack geometries, the estimates of w_N are identical, i.e. 0.821. This is due to the relatively negligible contributions of the fatigue flaw size dimensions to the variance of logarithmic fatigue life. Based on the estimate of w_N, 90% prediction limits (N^p - VMEA - mean) were determined, see the cyan dashed curves in Figure 4. The considered variation in input for the best-estimate flaw tolerance analysis may thus result in a variation of the estimated propagation fatigue life with a factor of almost 4 starting from the mean estimate. It may be noted that the 90% prediction limits include the data points of the experimental study in [5], which gives support for the best-estimate flaw tolerance approach to relatively accurately predict the total fatigue life with a fracture mechanical analysis based on a postulated initial fatigue flaw.

Table 7 Contributions to the coefficient of variation of propagation fatigue life.

Variables		Coefficient of variation	Internal flaw		External flaw	
j	x_j	w_j	c_j	τ_j^2	c_j	τ_j^2
1	$\|\varepsilon_a\|_m$	0.2	-3.3	0.436	-3.3	0.436
2	C	0.45	-1	0.203	-1	0.203
3	a	0.5	-0.271	0.018	-0.258	0.017
4	l	0.5	-0.265	0.018	-0.278	0.019
Variance of logarithmic fatigue life, $s_{\ln N}^2 (\approx \boldsymbol{w}_N^2)$				0.674		0.674
Standard deviation of logarithmic fatigue life, $s_{\ln N} (\approx w_N$, coefficient of variation of fatigue life)				**0.821**		**0.821**

7 Discussion

Fatigue flaw tolerance assessments are expected to yield a conservative estimate of total fatigue life by modelling fatigue crack propagation only. Initiation or nucleation fatigue life is then neglected, as well as fatigue crack propagation up to the postulated initial flaw size. Additionally, in the current investigation, the number of cycles consumed by fatigue crack growth for $a \geq 0.8t$, are also neglected. Besides the limits imposed on the fatigue flaw size, the use of conservative estimates or upper-bounds of the material parameters for the fatigue crack growth law also contribute to the overall conservatism of the flaw tolerance assessments. Indeed an increased fatigue growth law factor or exponent induces larger crack growth rates, which yields shorter estimated fatigue life.

The performed sensitivity analysis illustrated the importance of the load description for the results from the flaw tolerance assessment. Several assumptions related to the load description are intended to ensure the inherent conservatism of the used procedures. First, the load description is based on elastic pseudo-stress. Any reduction in stress due to local plastic deformation is thus neglected, although inelastic deformations are definitely expected to have occurred in the vicinity of the welding joint during fatigue testing [5]. Hence, a reduction of the stress intensity factor range due to plasticity is not accounted for, which will induce larger crack growth rates. Furthermore, the performed fatigue flaw tolerance assessments assume absence of crack closure effects on the fatigue crack growth rate. This assumption also ensures conservatism of the estimated fatigue life, as crack closure is expected to have occurred during the performed fatigue experiments in [5]. Using the entire stress intensity factor range is then an over-estimation of the fatigue crack driving force. Conservatism of the fatigue flaw tolerance assessment may be reduced with the use of an effective measure [12]. Finally, the VA load spectra applied during testing, such as VAP and VAG, included many load cycles with small amplitudes. Initially during the damage process, these load cycles may not have contributed to fatigue crack growth, however at a later stage when the crack propagated due to the larger load cycles included in the load spectrum, these same small load cycles may start to gradually contribute to the damage process by participating in driving fatigue crack propagation. Such sequence or history effects are also expected to have occurred during fatigue testing with VA loads. The fatigue flaw tolerance assessments assume however conservatively that all load cycles, including thus even the smallest load cycles, contributed to fatigue crack growth propagation during the entire damage process, by setting the threshold ΔK_{th} to zero.

The load description is based on a load model using a constant stress concentration factor K_t and a normalized through-thickness evolvement of the stress concentration F, which were derived by FE analyses assuming a specific weld joint geometry. These quantities define how much the local stress field in the vicinity of the weld differs from the nominal stress field away from the welding joint. The load model also neglects the effect of the local stress field varying in the circumferential direction. The stress concentration actually occurring in the test specimens will therefore to some extent differ from the description used in the flaw tolerance assessments. The stress concentration factor is however expected to primarily affect the stress field near the initiation surface. Consequently, its effect at advanced fatigue crack growth can be considered to be relatively small. The assumed through-thickness evolvement F may also differ from reality, as for instance increased cap height will reduce the stress in the vicinity of the capping and thus directly affect F. The load model in the current investigation did furthermore not consider the weld residual stress. The through-thickness residual stress field will however directly affect the mean load, i.e. the load ratio R, which is expected to influence the fatigue crack growth rate in the flaw tolerance

assessments. A tensile weld residual stress will induce an increase in load ratio, which can give an increased fatigue crack growth rate, especially when R becomes positive with the fatigue growth law defined in ASME XI [4]. Tensile weld residual stresses can for the considered butt weld and pipe geometry be expected on the inside of the component. A reduction of the estimated propagation fatigue life can thus be expected for the internal fatigue flaw. The importance of this effect will depend on the relative importance of the weld residual stress magnitude compared to the magnitude of the stresses introduced by the external load. The load model is nevertheless considered as adequate for the investigation of the piping component, although some uncertainties about the actual effect of the weld joint geometry and the importance of the weld residual stress field remain and could potentially yield non-conservatism of the adopted assumptions.

The flaw tolerance approaches performed in the current investigation are based on the applicability of LEFM, which is not valid for short or small cracks, as they may present increased crack growth rates when compared to long or large cracks [12]. A crack can furthermore be physically, mechanically or microstructurally small, when the crack size is less than, or of comparable size as a characteristic dimension or limit:

- A crack is typically considered as physically small when the crack size is less than 1 mm.
- A crack is referred to as microstructurally long or large when its size is significantly larger than a characteristic dimension of the microstructure [12], such as the average grain size, dg. For the considered austenitic stainless steel, dg ≈ 40 μm, which is to be compared to the initial crack depth used in the flaw tolerance approach.
- A crack with a size comparable to the cyclic plastic zone radius, rpc, at the crack tip is referred to as mechanically small [12]. The initial crack depth is then compared to the cyclic plastic zone size radius, which can be estimated under plane strain conditions [9] by

$$r_{\mathrm{pc}} \approx \frac{1}{6\,\pi}\left(\frac{\Delta K}{2\,\sigma_{\mathrm{yc}}}\right)^2 \tag{25}$$

  The estimates of r_{pc} for the different analyses performed in the current investigation are summarized in Table 8 and based on the total stress intensity factor range, computed neglecting crack closure effects and considering the initial flaw size.

Table 8 Characteristic dimensions for the microstructure and cyclic plastic zone size depending on the considered crack geometry and flaw tolerance approach.

Characteristic dimension	Crack geometry or initiation location	Flaw tolerance assessment	
		Standard	Best-estimate
d_{g} [μm]		40	
r_{pc} [μm]	Internal	65	55
	External	86	68

The results in Table 8 indicate that the cyclic plastic zone size radius is always larger than the average grain size diameter, which is typical for the Paris regime of fatigue crack growth [12], where Equation (1) is assumed valid. The postulated initial flaw depth, see Table 2, is less than 1 mm for the best-estimate approach, but the initial flaw length exceeds 1 mm. The crack is then considered as physically short, but not small. For the standard approach the initial flaw is considered physically large. Comparison of the initial crack depths postulated for the different flaw tolerance assessments with d_g indicates that the initial fatigue flaws may be considered as microstructurally long. Considering the initial a/l ratio of 1/6, the crack front of the initial planar semi-elliptical crack will cover in average at least 6 times more grains than along the initial crack depth. Consequently microstructural effects on the simulated fatigue damage process may be assumed negligible. Furthermore, are the initial flaw sizes larger than the cyclic plastic zone radius. The margins may be considered sufficient for the standard flaw tolerance approach, but are limited for the best-estimate approach and in particular when considering initiation from outside. The initial crack depth is then indeed slightly larger than 7 r_{pc}. The used approach in the current study assumed LEFM to be applicable, which may be questioned for the best-estimate approach. The computed crack growth rates may thus under-estimate the actual crack growth rates experienced by the physically or mechanically short cracks, which is a source of potential non-conservatism. The effect of increased crack growth rates related to short cracks is nevertheless studied through variation of the fatigue growth law factor in the sensitivity analysis, which underlines the importance of estimating the variation of the computed fatigue life.

An estimate of the total fatigue life is thus obtained by the performed assessments based on multiple assumptions related to the initial flaw size, the fatigue growth law parameters and the load description. The assumptions induce in general conservatism, but some potential sources for non-conservatism remain. These are related to the applicability of LEFM to short cracks, the effects of the weld residual stress field and uncertainties about the actual local stress field prevailing in the vicinity of the weld. Comparison between the experimental total fatigue life and the computed estimate of the fatigue life informs about the actual margins and degree of overall conservatism for the considered flaw tolerance approach. The results in Figure 4 show that the standard flaw tolerance approach inspired by ASME XI [4] always yields a conservative estimate. The estimate is for the considered experiments always considerably less than 10% of the actual number of cycles resulting in failure of the investigated piping component, see also Figure 5. This would imply that at least 90% of the total fatigue life is consumed by initiation. The best-estimate approach, which used an initial flaw size and fatigue growth law factor reduced with approximately 1/3, yielded estimation of the total fatigue life presenting a significant reduction and for larger loads even loss of overall conservatism. This is related to the mentioned potential sources for non-conservatism, but is compensated by the additional sensitivity analysis, which yielded 90% prediction limits bounding the data points of the experimental study in [5], see Figure 4. The results of the best-estimate approach imply a negligible contribution of initiation fatigue life to the total fatigue life of the performed experiments. The estimated lower and upper 90% prediction limits represent approximately a factor 15 in fatigue life, which informs about the variability in computed estimates given a certain variation in selected input variables. The performed VMEA indicates a predominant role of the load magnitude in the variation of the predicted total fatigue life. This observation highlights the importance of accurate load description for fatigue flaw tolerance assessments, in order to reduce variation in the computed fatigue life estimate. The material description through the fatigue growth law factor will also give a non-negligible contribution to the variation in assessment output, when the variation in load does

not exceed the one in the fatigue growth law factor. These results are based on a VMEA considering only a selection of four independent variables. The effects of the fatigue growth law exponent, elastic material properties or the nominal pipe geometry were not considered explicitly, in order to simplify the analyses by avoiding dependencies between variables. Their effect was however to some extent included by assuming increased variation of their dependent variables.

8 Conclusions

The current investigation examined fatigue flaw tolerance approaches based on fracture mechanical analyses used to estimate fatigue life and determine service intervals for components. The investigation considered the welded austenitic stainless steel piping component used in the experimental fatigue study in [5], and was performed using ProSACC (version 2.1 rev 2). It included a standard conservative approach inspired by Appendix L in ASME XI [4], and a best-estimate approach with a sensitivity analysis. The main findings of the current investigation considering both an internal and external fatigue flaw are:

- The conservative ASME inspired fatigue flaw tolerance approach yields extensive conservatism and consequently implies that an extensive part of at least 90% of the fatigue life is consumed by fatigue nucleation.
- Conservatism is significantly reduced and may even be lost for the best-estimate flaw tolerance approach, which implied a negligible contribution of fatigue initiation to the total fatigue life.
- Assumptions related to neglecting tensile weld residual stress fields, applying LEFM to short or small cracks and uncertainties about the actual local stress field prevailing in the vicinity of the weld joint constitute potential sources of non-conservatism in the estimate of total fatigue life.
- Overall conservatism of the fatigue flaw tolerance approach is preserved by assuming a relatively large initial flaw size and neglecting effects from inelastic material behavior, sequence effects for variable amplitude loads and crack closure effects. Conservatism may also be introduced or extended by selecting increased fatigue growth law parameters.
- Variation of selected input data covering initial crack geometry, growth law and load description induced relatively large variability of the estimated fatigue life, but the estimated 90% predictions limits contained the experimental results.
- The VMEA indicated that the extent of the variability of the estimated fatigue life is primarily due to the variation or uncertainty in load and to some minor extent also to the fatigue growth law parameters.
- The coefficient of variation of the estimated fatigue life is expected to rapidly exceed unity for increasing uncertainty in load. Load measurement or monitoring programs may contribute to accurate or relevant load description enabling significant reduction of the variability of the output of the fatigue flaw tolerance approach.

The results support the use of flaw tolerance approaches for demonstrating reliability of a component using fracture mechanics methods, although the choice of input data is shown to strongly affect the overall degree of conservatism for the obtained fatigue life estimate. The performed work has contributed to verification of flaw tolerance approaches used in industry, which will facilitate the choice of optimal and safe control intervals for components subjected to fatigue loads.

9 Recommendations

During the course of the current investigation, some limitations were observed, which may be resolved by considering the following actions:

- Small postulated initial fatigue flaws were assumed, but considering the relatively small wall thickness of the considered component, the postulated initial crack depths were relatively large compared to the wall thickness. As a result the extent of actual simulated fatigue crack growth was fairly small compared to the wall thickness. A similar investigation considering a thick-walled piping component would be valuable to confirm the obtained results and allow generalization to a broader range of piping components than the considered specific welded piping geometry.
- The VMEA provided valuable information on variation in the computed fatigue life estimate and the relative contributions due the uncertainty related of each input parameter. The analysis considered though only a few independent variables. A more extensive sensitivity analysis can be performed by also including other dependent variables, such as the nominal pipe geometry, fatigue growth law exponent, stress concentration factor, etc.
- The used load model presented some limitations, amongst which the omission of the contribution of the weld residual stress. The magnitude of the weld residual stress field may be determined and its effect on the load ratio can be investigated. This study would aim at evaluating the error introduced by neglecting its contribution in the performed flaw tolerance approaches.

10 Acknowledgement

The Swedish Radiation Safety Authority is gratefully acknowledged for the financial support.

11 References

[1] ASME, "Boiler and Pressure Vessel Code, Section III, Rules for Construction of Nuclear Facility Components," 2013.

[2] O. Chopra and W. Shack, "Effect of LWR Coolant Environments on the Fatigue Life of Reactor Materials," NUREG/CR-6909, 2007.

[3] D. J. Dewees, P. Hirschberg, W. Reinhardt, G. L. Stevens, D. H. Roarty, S. Gosselin, K. Wright and T. M. Damiani, "ASME Section III Flaw Tolerance Sample Problem for Fatigue Design of Nuclear System Components," in *Proceedings of the ASME 2014 Pressure Vessels & Piping Conference*, Anaheim, 2014.

[4] ASME, "Boiler and Pressure Vessel Code, Section XI, Rules for Inservice Inspection of Nuclear Power Plant Components," 2013.

[5] M. Dahlberg, D. Hannes and T. Svensson, "Evaluation of fatigue in austenitic stainless steel pipe components," SSM 2015:38, 2015.

[6] D. Hannes, M. Dahlberg and Z. Chen, "Fatigue fracture surface characterization and investigation," Submitted to SSM, 2016.

[7] T. Svensson, D. Hannes, P. Johannesson, M. Dahlberg and A. Anderson, "Three HCF models for strain fatigue life of welded pipes in austenitic stainless steel," *Procedia Engineering,* vol. 101, pp. 476-484, 2015.

[8] P. Dillström, M. Bergman, B. Brickstad, W. Zang, I. Sattari-Far, P. Andersson, G. Sund, L. Dahlberg and F. Nilsson, "A combined deterministic and probabilistic procedure for safety assessment of components with cracks - Handbook," SSM 2008:01, 2008.

[9] P. Ljustell, "Fatigue crack growth experiments on specimens subjected to monotonic large scale yielding," *Engineering Fracture Mechanics,* vol. 110, pp. 138-165, 2013.

[10] J.-H. Baek, Y.-P. Kim, W.-S. Kim and Y.-T. Kho, "Fracture toughness and fatigue crack growth properties of the base metal and weld metal of type 304 stainless steel pipeline for LNG transmission," *International Journal of Pressure Vessels and Piping,* vol. 78, pp. 351-357, 2001.

[11] ANSYS, Inc., "User manual," ANSYS, Release 14.5.

[12] S. Suresh, Fatigue of Materials, Cambridge University Press, 2001.

[13] B. Bergman, J. de Maré, S. Lorén and T. Svensson, Robust Design Methodology for Reliability, John Wiley & Sons, Ltd., 2009.

2016:27

The Swedish Radiation Safety Authority has a comprehensive responsibility to ensure that society is safe from the effects of radiation. The Authority works to achieve radiation safety in a number of areas: nuclear power, medical care as well as commercial products and services. The Authority also works to achieve protection from natural radiation and to increase the level of radiation safety internationally.

The Swedish Radiation Safety Authority works proactively and preventively to protect people and the environment from the harmful effects of radiation, now and in the future. The Authority issues regulations and supervises compliance, while also supporting research, providing training and information, and issuing advice. Often, activities involving radiation require licences issued by the Authority. The Swedish Radiation Safety Authority maintains emergency preparedness around the clock with the aim of limiting the aftermath of radiation accidents and the unintentional spreading of radioactive substances. The Authority participates in international co-operation in order to promote radiation safety and finances projects aiming to raise the level of radiation safety in certain Eastern European countries.

The Authority reports to the Ministry of the Environment and has around 300 employees with competencies in the fields of engineering, natural and behavioural sciences, law, economics and communications. We have received quality, environmental and working environment certification.

Strålsäkerhetsmyndigheten
Swedish Radiation Safety Authority

SE-171 16 Stockholm
Solna strandväg 96

Tel: +46 8 799 40 00
Fax: +46 8 799 40 10

E-mail: registrator@ssm.se
Web: stralsakerhetsmyndigheten.se